Photometry and Transit Modeling of Exoplanet XO-1b

Simon Sikora
Adlai E. Stevenson High School, 1 Stevenson Drive, Lincolnshire, IL 60069

Timothy Banks
Department of Physical Science and Engineering, Harper College, 1200 W. Algonquin Road, Palatine, IL 60067, and Data Science, Nielsen, 200 W. Jackson, Chicago, IL 60606; tim.banks@nielsen.com

Received September 16, 2022; revised September 4, 2023; accepted September 6, 2023

Abstract CCD images of transits by the exoplanet XO-1b over the years 2018 to 2021 are analyzed. The data were collected by a MicroObservatory telescope in Arizona. These are supplemented by analysis of TESS space telescope data along with transits observed by amateur astronomers, leading to an investigation of the mid-transit times and the orbital period of the exoplanet. No evidence is found to support transit timing variations, with a period of 3.9415049 ± 0.0000008 days being sufficient to explain mid-transit times over 2006 to 2021. Using TESS data, the orbital radius is estimated to be some 11.10 ± 0.15 times the radius of the host star, and the planetary radius 0.1300 ± 0.0016 times the stellar radius. A simple transit model is combined with Bayesian sampling to provide estimates for the orbital inclination, radii, and limb darkening, however these estimates are not internally consistent. This is likely due to the application of the "small planet approximation," which neglects a radial gradient in the stellar flux obscured by the planet (due to the limb darkening effect), together with the model not accounting for variation in the stellar flux.

1. Introduction

The study of exoplanets, via transits, is an appealing field for students who can contribute to the rapidly growing scientific knowledge of such systems. Banks *et al.* (2020) outlined a research program involving undergraduate students analysing transit and radial velocity data for exoplanets, and commented that such programs are ideal for astronomical outreach projects. Not only were students able to conduct meaningful and publishable research, they were able to expand their skill sets such as in computer programming through building models from first principles and implementing optimization techniques. Such skills are marketable and valuable in the commercial world, with these projects building up not only the students' interest in, and support of, astronomy but also skills for the wider workplace. Banks *et al.* ended their paper suggesting that such programs could be possible for final year high school students. The current paper outlines such an extension. It describes work by a high school student analyzing archival data, both images and reduced data, investigating the exoplanet XO-1b. The project aim was to estimate parameters such as planetary radius and orbital inclination for the system as well as model the period of the system, searching for variations in the mid-transit timings that could indicate the gravitational effect of another currently unknown (and non-transiting) planet or planets. Such variations are known as TTVs, or Transit Timing Variations.

F. Sienkiewicz of the Harvard-Smithsonian Center for Astrophysics (CfA) suggested the study of the exoplanet XO-1b (orbiting the host star also known as BD+28 2507, which has ICRS (2000) coordinates $\alpha = 16{:}02{:}11.8$, $\delta = +28{:}10{:}10.4$), using imagery from the CfA's MicroObservatory (MObs) which he kindly supplied to the authors. This transiting exoplanet was discovered by the XO project (McCullough *et al.* 2006), with confirmation later that year by SuperWASP-North (Wilson *et al.* 2006). The planet's mass is estimated to be ~0.9 times that of Jupiter, completing an orbit in $3.9415160^{+0.0000230}_{-0.0000250}$ days (Patel and Espinoza 2022) at a distance of ~ 0.49 astronomical unit. "Surface" temperatures are estimated at around 1200 Celsius, leading to XO-1b being identified as an example of the "Hot Jupiter" class of exoplanets.

2. Data Analysis

2.1. MicroObservatory

The analyzed observations were taken by a 6-inch aperture MicroObservatory (MObs; Sadler *et al.* 2001) telescope. This automated telescope is located at Mount Hopkins in Arizona (latitude 31.675°, longitude –110.952°, and a 1,268-m altitude above sea level). 60-second long exposures were collected using a KAF-1403 ME CCD camera. The CCD has a pixel scale of 5.2 arcseconds. 2 × 2 binning was applied to the images to reduce noise. No filters were used in the observations, i.e., the images were in white light.

The software EXOTIC (Zellem *et al.* 2020) was used to reduce the transit data. This is PYTHON software developed by the Jet Propulsion Laboratory's "Exoplanet Watch" program. It can run on a variety of different operating systems (as a PYTHON library) and is also available online inside Google's "Colaboratory" (This is how Google spells the name for this tool). EXOTIC is intended for the analysis of individual transits, processing science frames through calibration and photometric measurement to the final fitting of a transit light curve model using Markov Chain Monte Carlo (MCMC) for optimization. EXOTIC can be used to reduce the images collected during a transit after the event, or process science images as they are acquired during a transit. If calibration frames are available (such as flat field, dark, and bias images), EXOTIC will automatically apply these to the science images as part of its data reduction before performing differential photometry. The user will select a number of possible comparison stars, which EXOTIC evaluates for stability (excluding any "comparison" stars with observed variability). The software can also be used to model observed

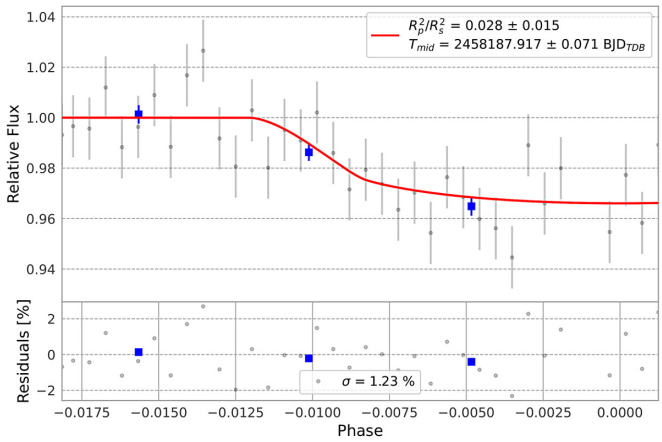

(a) 13 March 2018

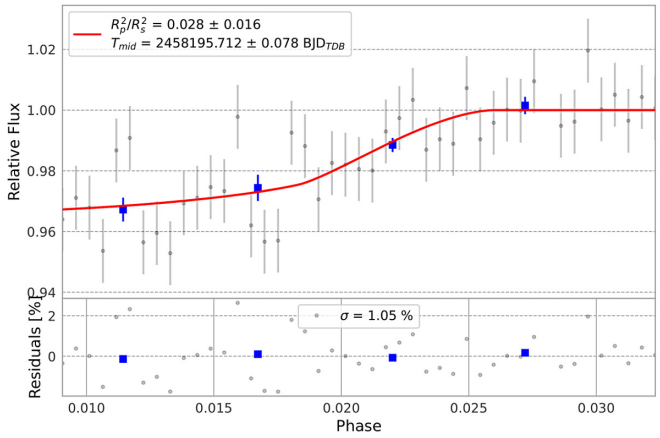

(b) 17 March 2018

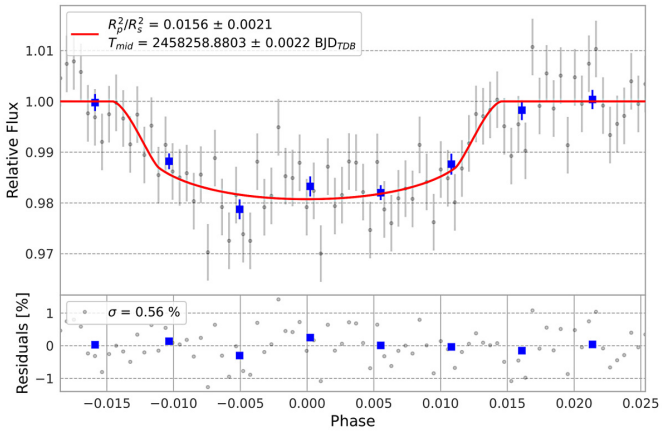

(c) 20 May 2018

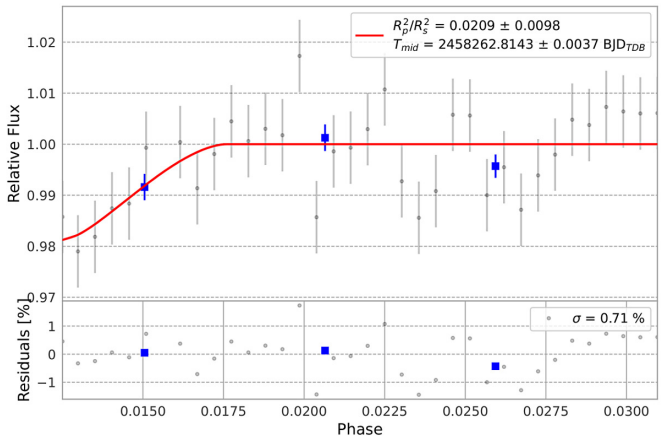

(d) 24 May 2018

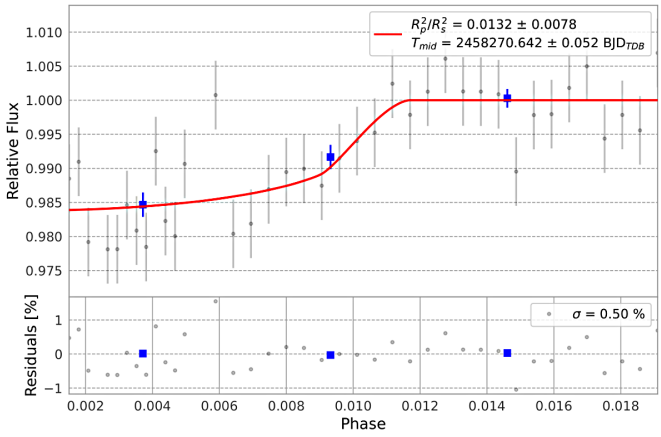

(e) 31 May 2018

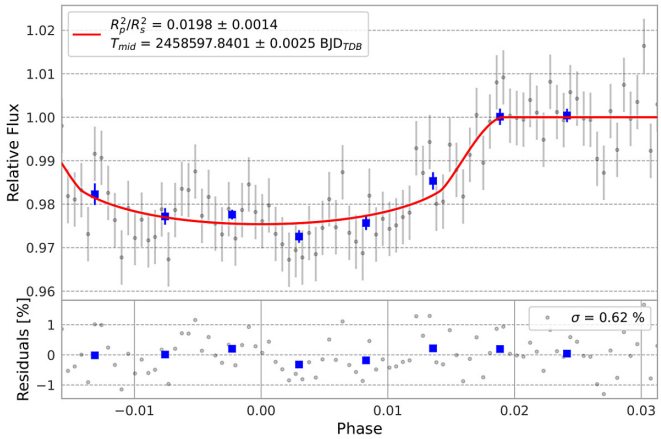

(f) 24 April 2019

Figure 1. MicroObservatory XO-1b transit data and models. The red lines show the expected variation based on the best fitting exotic model for each transit.

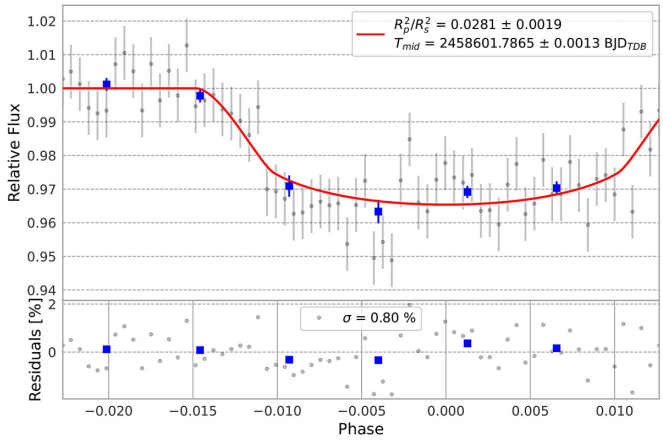

(g) 28 April 2019

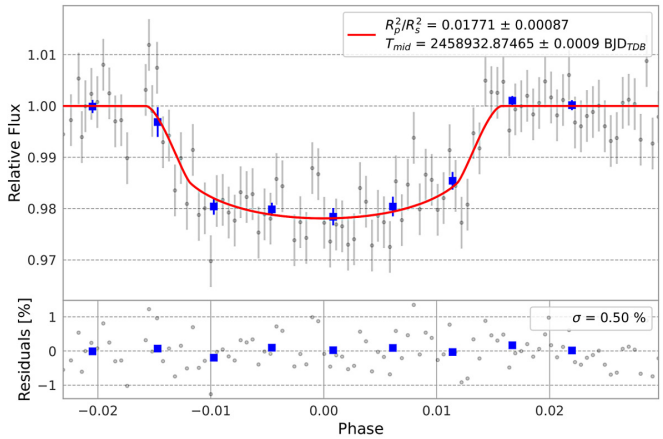

(h) 23 March 2020

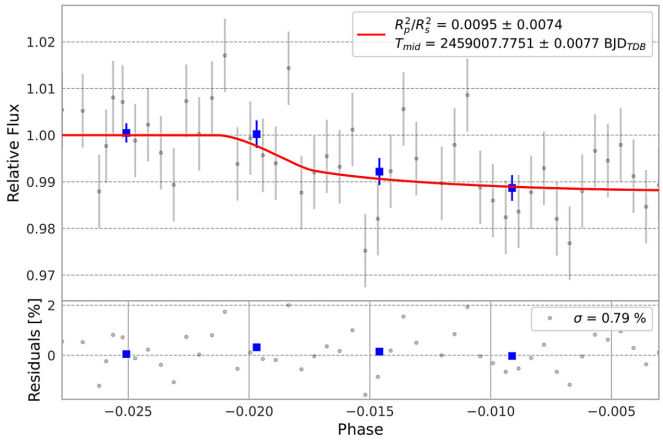

(i) 07 June 2020

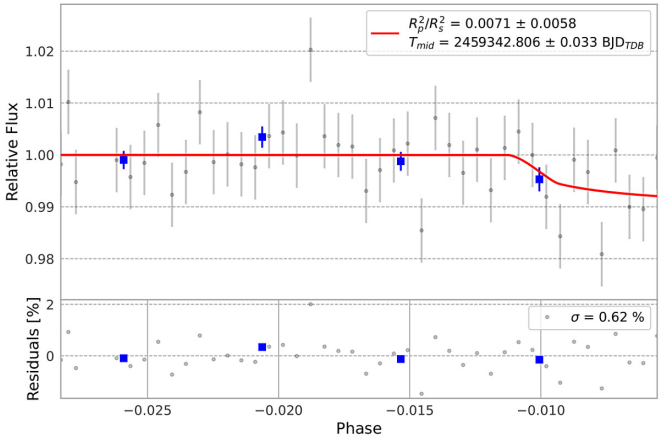

(j) 12 May 2021

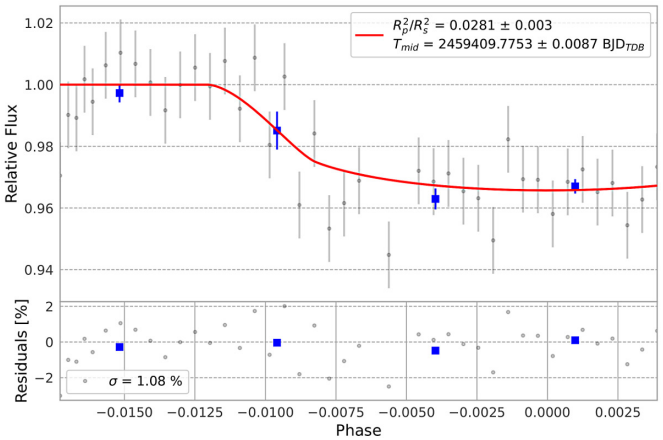

(k) 18 July 2021

Figure 1. MicroObservatory XO-1b transit data and models, cont.

Table 1. Fitted Parameters for XO-1b from the EXOTIC modelling.

Date	*Mid-transit*	a/r_s	r_s/a	r_p/r_s	*Quality*	*Source*
14 March 2006	2453808.9158 ± 0.0003	11.420 ± 0.084	0.0876 ± 0.0006	0.1296 ± 0.0012	Complete	Bruce Gary, Arizona
01 June 2006	2453887.74685 ± 0.00037	11.160 ± 0.081	0.0896 ± 0.0007	0.13223 ± 0.00096	Complete	Bruce Gary, Arizona
24 July 2007	2454214.89356 ± 0.00049	11.09 ± 0.11	0.0902 ± 0.0009	0.1346 ± 0.0010	Complete	Bruce Gary, Arizona
28 March 2008	2454553.85823 ± 0.00041	10.485 ± 0.085	0.0954 ± 0.0008	0.1314 ± 0.0011	Background uneven	Bruce Gary, Arizona
03 June 2008	2454620.86759 ± 0.00043	11.106 ± 0.087	0.0900 ± 0.0007	0.1342 ± 0.0009	Complete	Cindy Foote, Utah
07 June 2008	2454624.8118 ± 0.0009	11.76 ± 0.23	0.0850 ± 0.0017	0.1317 ± 0.0023	Complete	Cindy Foote, Utah
11 June 2008	2454628.7484 ± 0.0035	10.95 ± 0.60	0.0913 ± 0.0050	0.1307 ± 0.0014	Partial	Bruce Gary, Arizona
02 May 2009	2454963.7784 ± 0.0004	11.273 ± 0.082	0.0887 ± 0.0006	0.12550 ± 0.00077	Complete	Bruce Gary, Arizona
13 May 2009	2454983.4856 ± 0.0005	11.29 ± 0.12	0.0886 ± 0.0009	0.1315 ± 0.014	Complete	Jose Gregorio, Portugal
16 May 2009	2454967.71796 ± 0.00040	10.928 ± 0.095	0.0915 ± 0.0008	0.13295 ± 0.00098	Complete	Bruce Gary, Arizona
20 May 2009	2454971.65900 ± 0.00045	10.801 ± 0.005	0.09258 ± 0.00004	0.13576 ± 0.00093	Almost complete	Bill Norby, Missouri
13 March 2018	2458187.917 ± 0.061	14.88 ± 2.29	0.067 ± 0.010	0.167 ± 0.045	Partial	MObs
17 March 2018	2458195.712 ± 0.078	7.12 ± 1.56	0.140 ± 0.031	0.166 ± 0.047	Partial	MObs
20 May 2018	2458258.8803 ± 0.0022	11.99 ± 0.78	0.083 ± 0.005	0.1249 ± 0.0084	Complete	MObs
24 May 2018	2458262.8143 ± 0.0037	10.21 ± 1.77	0.098 ± 0.017	0.144 ± 0.034	Very partial	MObs
31 May 2018	2458270.642 ± 0.005	14.62 ± 2.26	0.068 ± 0.011	0.115 ± 0.034	Partial	MObs
24 April 2019	2458597.8401 ± 0.0025	9.42 ± 0.36	0.106 ± 0.004	0.1407 ± 0.0048	Almost complete	MObs
23 April 2019	2458601.7865 ± 0.0013	12.28 ± 0.38	0.081 ± 0.003	0.1677 ± 0.0056	Almost complete	MObs
23 March 2020	2458932.8746 ± 0.0009	11.23 ± 0.19	0.089 ± 0.002	0.1331 ± 0.0033	Complete	MObs
21 April 2020	2458960.46415 ± 0.00037	11.120 ± 0.076	0.0899 ± 0.0006	0.12896 ± 0.00081	Complete	TESS
24 April 2020	2458964.40590 ± 0.00036	11.118 ± 0.079	0.0899 ± 0.0006	0.13070 ± 0.00079	Complete	TESS
06 May 2020	2458976.22962 ± 0.00036	11.104 ± 0.075	0.0901 ± 0.0006	0.13030 ± 0.00079	Complete	TESS
10 May 2020	2458980.16968 ± 0.00035	11.062 ± 0.075	0.0904 ± 0.0006	0.13007 ± 0.00078	Complete	TESS
07 June 2020	2459007.7751 ± 0.0077	8.13 ± 1.97	0.123 ± 0.030	0.098 ± 0.038	Partial	MObs
12 May 2021	2459342.806 ± 0.033	14.17 ± 2.34	0.068 ± 0.011	0.084 ± 0.034	Very partial	MObs
18 July 2021	2459409.7753 ± 0.0087	14.89 ± 1.76	0.067 ± 0.008	0.1676 ± 0.0089	Partial	MObs

Notes: Mid-transit times are given in Barycentric Julian Dates (Barycentric Dynamical Time), the orbital semi-major axis (a) in terms of the stellar radius (r_s), and the planetary radius (r_p) relative to the stellar radius. exotic outputs a/r_s, so a column giving the inverse is given for convenience when comparing with a later model and the literature. Uncertainties are 1σ "MObs" indicates the source is the MicroObservatory telescope described in the text, "TESS" indicates this space telescope, and for amateur-contributed data the name of the observer and their general location is given. The amateur-contributed data were sourced from the NASA Exoplanet Archive.

fluxes, such as obtained through other reduction packages for photometry, and fit a transit model (as we will see below for data from the TESS space telescope). EXOTIC automatically scrapes "priors" for the MCMC fitting from the online NASA Exoplanet Archive (NEA; Akeson *et al.* 2013). "Priors" are assumed probability distributions based on previous (prior) experience. Limb darkening values are taken from EXOFAST (Eastman *et al.* 2013).

The MicroObservatory observations included only science frames and dark images. No flat fields were collected, while the dark frames were collected at the beginning and end of the observations each night. We followed the reduction process outlined by North and Banks (2022).

The results from the EXOTIC fitting are given in Table 1. Figure 2 plots the observations for each fit together with the model estimated by EXOTIC. There were only 2 complete transits observed out of the 11 clear nights. The other 9 attempts were partial transits, which led us to consider that perhaps XO-1b was subject to transit timing variations (TTV). We expected the telescope time to be scheduled such that the transit would be within the planned observation period. Partial transits lead to greater estimated uncertainties. Additional complete transits could lead to confirmation whether XO-1b was subject to TTVs, which could explain why so many of the MObs observation sessions were actually incomplete observations of the transits. To explore this idea further we sourced additional data, namely from the TESS space telescope and from the NASA Exoplanet Archive.

2.2. TESS

The Transiting Exoplanet Survey Satellite (TESS; Ricker *et al.* 2014) has been operational since 2018. XO-1 was observed with a two-minute cadence by TESS over the period 16 April 2020 to 12 May 2020. Four transits were selected from this period, having data to each side of a complete transit. TESS data are of high quality (see Figure 2). Results of the EXOTIC fits can be found in Table 1. Taking arithmetic means across the four values, the planet radius (r_p) was estimated as 0.1300 ± 0.0016 times the radius of its host star (r_s), with the semi-major axis of the orbit (a) being 11.10 ± 0.15 times the stellar radius. By comparison, for the two complete MObs transits EXOTIC estimated a planetary radius of 0.1249 ± 0.0064 and 0.1331 ± 0.0033 stellar radii, within error of the estimate based on the TESS data. The orbital radius estimates from these MObs transits were 11.99 ± 0.78 and 11.23 ± 0.19, again within formal error of the estimate from the TESS data.

We also applied the algebraic transit model of Mandel and Agol (2002) to two of the TESS transits, in order to estimate the orbital inclination of the planet and the limb darkening (which are not available from EXOTIC). We prepared this in the R programming language and made use of the Hamiltonian Markov Chain Monte Carlo (MCMC) optimization method (hereafter abbreviated as HMC) as implemented in the STAN programming language (Carpenter *et al.* 2017; STAN Development Team 2022). Monte Carlo techniques are sampling methods. MCMC involves sampling from probability distributions using Markov chains. A Markov Chain is a

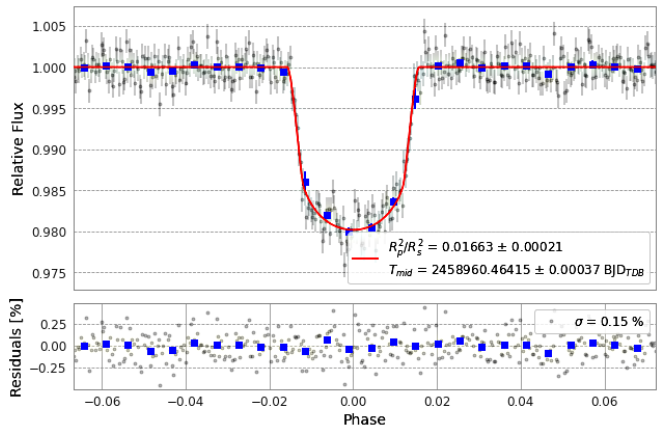

(a) 21 April 2020

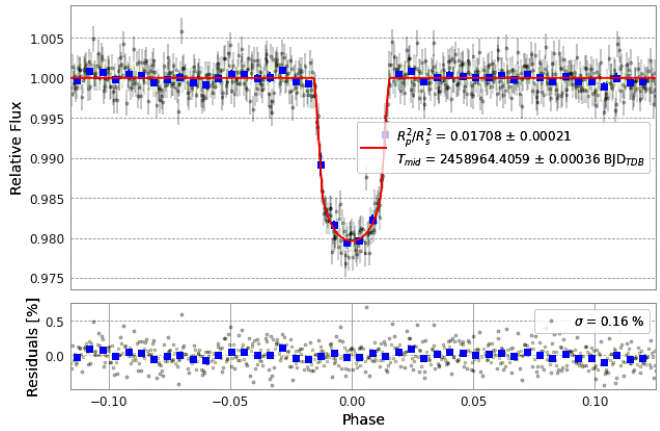

(b) 24 April 2020

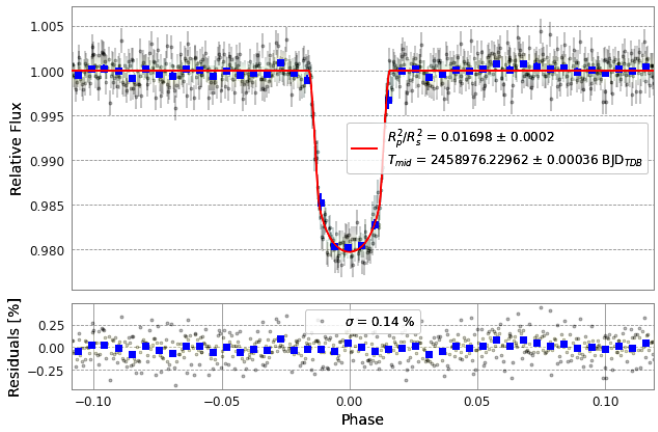

(c) 06 May 2020

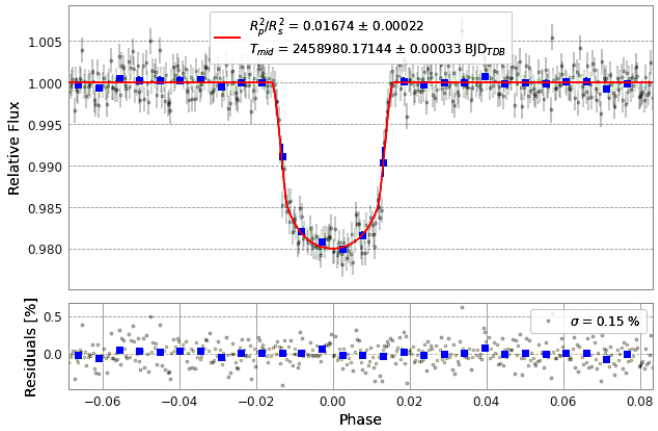

(d) 10 May 2020

Figure 2. TESS XO-1b transit data for four dates and best fit transit models. We used a different way of running exotic to model the TESS data. Instead of using a GUI-based wrapper for EXOTIC, we directly called exotic as a library inside a PYTHON program. This allowed us to input zero airmasses for the TESS data since the space telescope is outside the Earth's atmosphere. A downside was that we had no control of where the information box, giving output parameters, was placed on the charts.

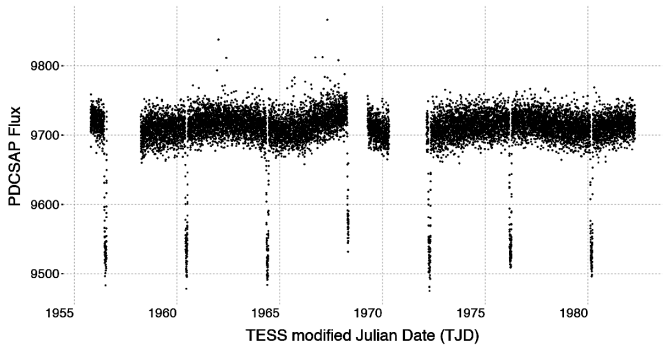

(a) TESS photometry

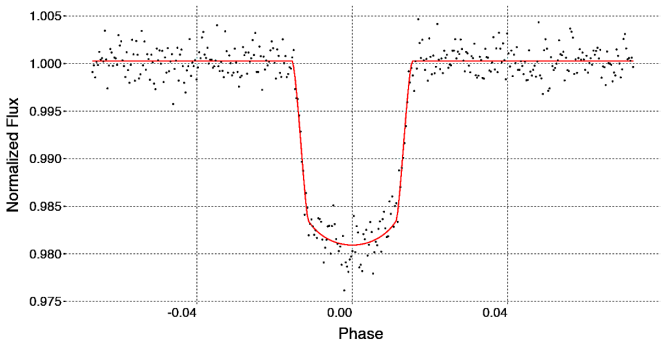

(b) 20 April 2020 transit

Figure 3. The figure on the left (a) shows the non-normalized Pre-search Data Conditioning Simple Aperture Photometry (PDC SAP) generated by the TESS team, which removed longstanding systematic trends and so provides better data quality than simple aperture photometry (also available from MAST). Exposures were 120-second and the data period covered 16 April 2020 to 12 May 2020. The relatively small variability of the host star is clearly visible. The figure on the right (b) shows one of these transits plus the optimal model generated by the HMC code. This transit is the first following the break in the data to the left of Figure 3a.

sequence of events, sampled from an unknown or target distribution, with each state depending only on the state of its immediate predecessor and not on earlier states. MCMC techniques allow the use of such chains to draw samples which are progressively more likely to represent the target distribution, explaining their use in optimization. A similar implementation was made by North and Banks (2022), where further details of the transit model and the MCMC technique can be found. We therefore refer the interested reader to that paper in *JAAVSO* for further details. MCMC takes a long time to run. Typically a single fit took several days to complete on the laptops we were using, explaining why we did not fit all of the available transits with this method.

The model of Mandel and Agol (2002) has the following parameters: r_p is the planetary radius relative to that of the host star (r_s), a is the orbital semi-major axis in terms of the stellar radius, u is the linear limb darkening co-efficient, cos i is the cosine of the orbital inclination, and L is the adjustment in normalized flux. The implementation of this model in HMC included the parameter σ, which is an estimate of the Gaussian noise, and "offset," which is the adjustment in phase.

Figure 3 displays the TESS photometry, together with one of the model transit fits to the TESS data. Figure 4 displays the "corner" or "pair" plot which was output by the HMC optimization. A pair plot like this allows comparisons between pairs of variables. The density plots in the upper left show the distribution of parameter estimates by the Markov chains for each of the pairs of variables, e.g., the sub-plot in the upper left corner plots the distribution of parameter estimates for the random noise σ (which is taken as a variable in the fitting model) and the planetary radius r_P. The color red indicates that many steps (or parameter estimates) were in this point, whereas green indicates that there were fewer steps at a point shaded with this color and is therefore a lower fit to the observed data. The histograms on the diagonal from lower left to upper right show the distributions of each of the fitting variables. Finally, the

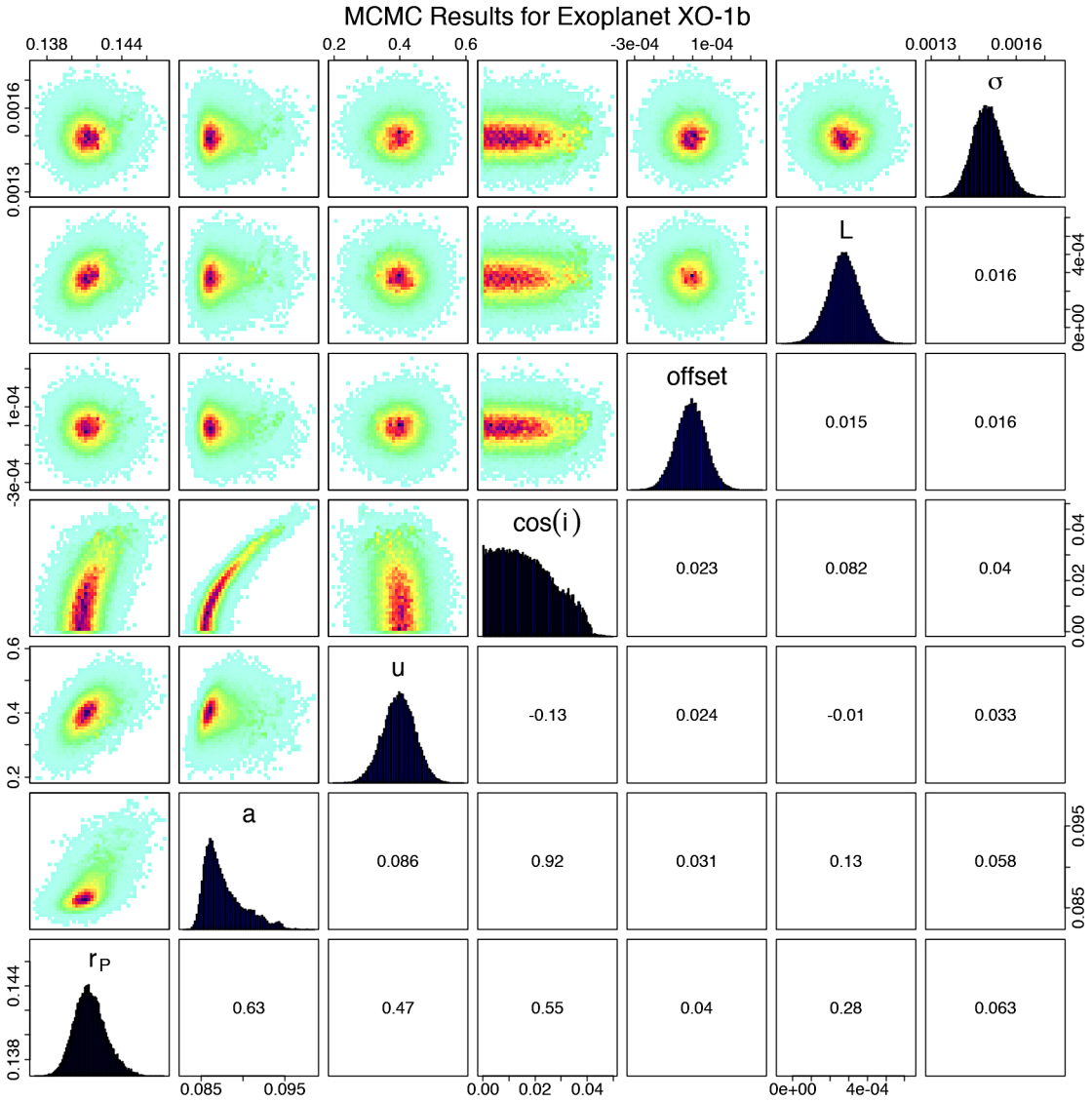

Figure 4. Pair-plot of the MCMC results for the 20 April 2020 transit of XO-1b. This represents 100,000 steps in each of the four Markov chains. An additional 50,000 steps (per chain) at the start of the optimization were excluded as "burn-in." The axes of the density plots are in the units of each parameter, as given in the text. The numbers in the lower right of the diagram are the Pearson correlation coefficients (R) for each pair of variables. This diagram was prepared using the base R programming language command "pairs."

correlations between the variables are given as the values in the boxes in the lower right. For example, we can see that the correlation between σ and the linear limb darkening u is close to zero (0.033), as we would expect. The figure is based on 100,000 steps by the chains, following the initial 50,000 steps of each chain being discarded. These initial steps are routinely discarded by MCMC practitioners since the starting parameters for the chains are likely to be far from the final optimal values. The parameter values therefore will trend as the optimizer steps towards the global minimum (best fitting values) and should be discarded from the error analysis.

Fitting the first modelled transit (second transit from the left in Figure 3a) resulted in r_p / r_s being estimated as 0.14161 ± 0.0006, $r_s / a = 0.0877 \pm 0.0007$, inclination i = 89.03 ± 0.04 degrees, and limb darkening u = 0.396 ± 0.001. Uncertainties are single sigma. The second transit (second from the right in Figure 3a) modelled using the HMC technique resulted in r_p / r_s being estimated as 0.14558 ± 0.0004, $r_s / a = 0.0922 \pm 0.0008$, inclination i = 88.26 ± 0.12 degrees, and limb darkening u = 0.451 ± 0.003. The formal uncertainties for the two sets of parameters do not, in general, overlap, suggesting that these formal one-sigma errors are under-estimates. This could partially be due to the stellar variations visible in Figure 3a, which was not accounted for in our modelling, together with a deficiency in the implemented model described below.

Our estimates for orbital inclination are in good agreement with the literature, e.g., 88.81 ± 0.50 degrees (Stassun *et al.* 2017), $88.81^{+0.70}_{-0.30}$ (Bonomo *et al.* 2017), 89.06 ± 0.84 (Southworth 2010), 88.8 ± 0.2 (Burke *et al.* 2010), $88.81^{+0.70}_{-0.30}$ (Torres *et al.* 2008), $89.31^{+0.46}_{-0.53}$ (Holman *et al.* 2006), 87.7 ± 1.2 (McCullough *et al.* 2006), and 88.92 ± 1.04 (Wilson *et al.* 2006). There is considerable variation in the literature estimates, in line with the HMC modeling.

Our HMC-based estimates for r_p are substantially larger than the literature, e.g., compared to 0.138 ± 0.020 (Wilson *et al.* 2006), 0.13102 ± 0.00064 (Holman *et al.* 2006), $0.1326^{+0.0004}_{-0.0005}$ (Torres *et al.* 2008), and $0.1315^{+0.0016}_{-0.0020}$ (Patel and Espinoza 2022) as well as our EXOTIC estimates. This leads to our estimates for r_p / r_s being correspondingly smaller than the literature and our EXOTIC estimates. We believe the problem lies in our use of the "small planet approximation," where we did not take into account the gradient of the limb darkening coefficient. Instead we took the limb darkening value corresponding to the centre of the planetary disc in front of the stellar disk, and applied this value across the entire obscured region. This appears to be too much of an approximation for XO-1b, which is a relatively large planet compared to its host star. Croll *et al.* (2007) noted that the small planet approximation is valid for $r_p = 0.1\ r_s$ and smaller. We therefore plan that future application of this simple model should be restricted to planets inside this limit, or the model be modified to account for the changing limb darkening values in the obscured regions. Despite this setback we have included the HMC analysis as a demonstration that motivated high school students can develop such analyses, as well as a "warning" for subsequent student research projects either to choose smaller planets relative to their stars or to integrate the limb-darkening flux to better account for the changes in limb darkening (particularly near the early ingress and late egress of the planet where limb darkening is at its greatest and so will impact estimates of the planetary radius). Modeling the stellar variation, such as through a Gaussian process (see Ng *et al.* 2021), would also be advisable.

2.3. NASA Exoplanet Archive

Light curves are available from the NASA Exoplanet Archive (NEA) which were collected by amateur astronomers and placed into the public domain. We examined the available data sets and selected those with complete or nearly complete transits, ignoring data sets that only partially covered the transits since we were primarily interested in as accurate as possible measurements of the mid-transit timings. Again, results from the EXOTIC fittings may be found in Table 1. Figure 5 presents the modelled data sets together with the light curves based on the best fitting models. The NEA fitted automatically a simple model to each dataset to estimate the mid-transit times (without a formal error being provided). The mean difference between the two methods (EXOTIC and NEA) was –49 ± 97 seconds, which is larger than we had hoped but reassuring that there is no significant difference from zero. We chose to model the period with the results from EXOTIC, as we believe this is a more complete transit model.

2.4. Period analysis

We performed regression analysis of the mid-transit times using R. A linear regression fitted the data well; no need for higher-order polynomial terms was required. We included the mid-transit timings of Bonomo *et al.* (2017), Patel and Espinoza (2022), and Kokori *et al.* (2022) to expand the data set. The period was estimated as 3.941498 ± 0.000008 days, using all available measurements. We subsequently restricted analysis to just complete and near complete transits, leading to a period estimate of 3.9415049 ± 0.0000008 days, which is outside the formal error range of the first estimate using all available data. Given the uncertainty of the fits to less complete data, we prefer the second period estimate. Our estimate is in good agreement with the literature values, e.g., $3.9415160^{+0.0000230}_{-0.0000250}$ days of Patel and Espinoza (2021), 3.941530 ± 0.000027 (Stassun *et al.* 2017), 3.9415128 ± 0.0000028 (Southworth 2010), etc.

Figure 6a shows the residuals from the linear fit to all available data, while Figure 6b shows the residuals from the fit to only complete or near complete transits. Figures 6c and 6d expand sections of the data shown in Figures 6a and 6b, respectively. There is no clear evidence for transit timing variations, with the formal uncertainties for the majority of residuals overlapping zero. However, there could be a bias introduced by our choice of only including complete transits for the earlier data. We therefore recommend that XO-1 continue to be monitored so that additional transits may be observed and timed. TTVs are therefore not the likely cause of the timing problems noted with the MObs data.

3. Discussion

We have presented reductions of 26 transit events for X0-1b, deriving an orbital period and finding no evidence for transit timing variations. Our estimates for the planetary and orbital

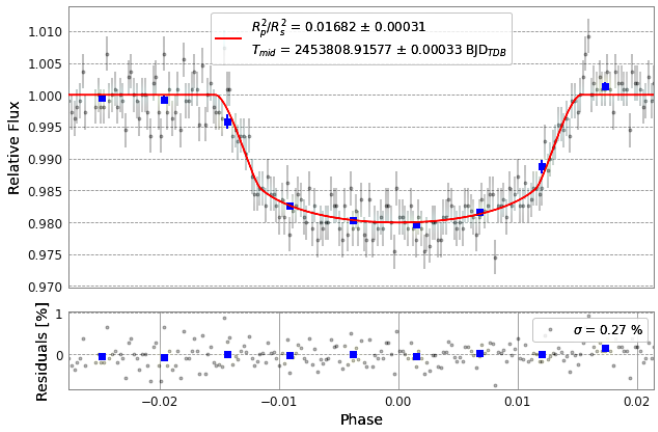

(a) 14 March 2006 (R)

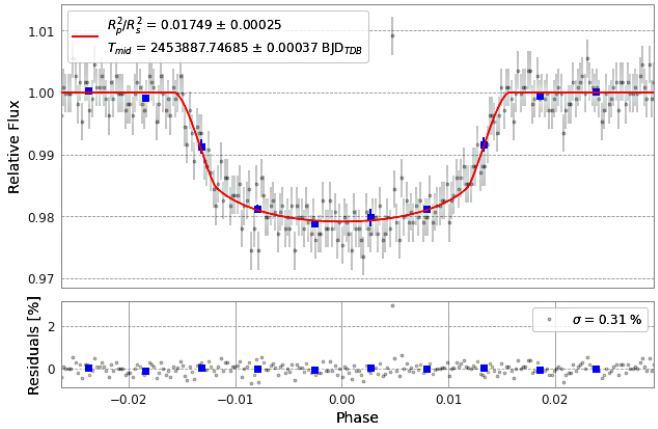

(b) 01 June 2006 (R)

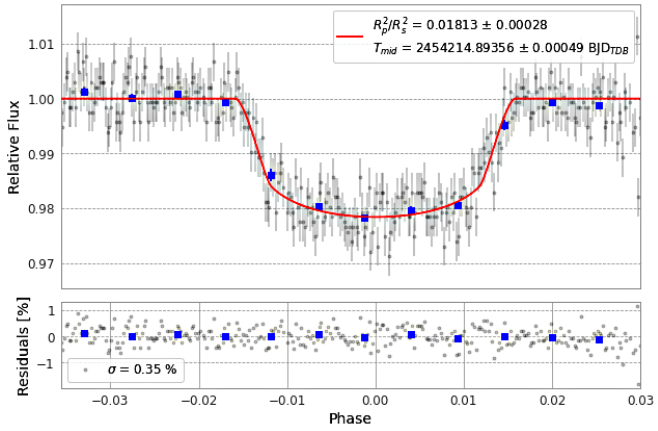

(c) 29 July 2007 (R)

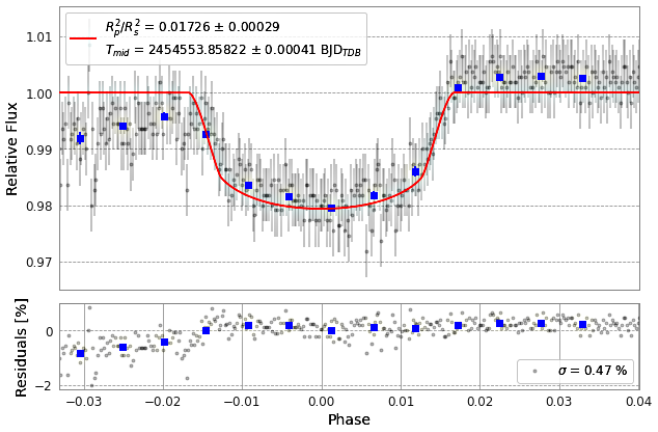

(d) 28 March 2008 (R)

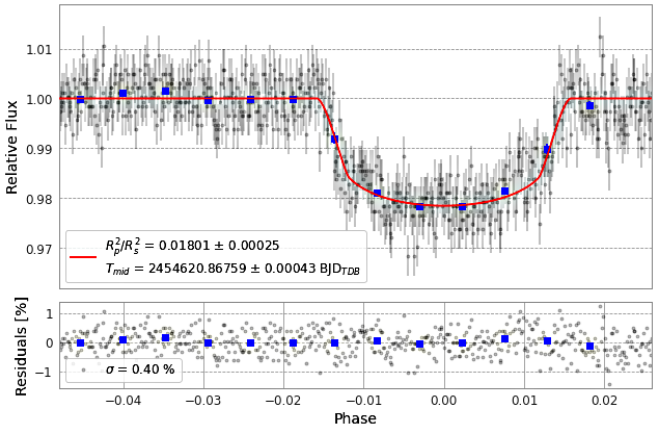

(e) 03 June 2008 (R)

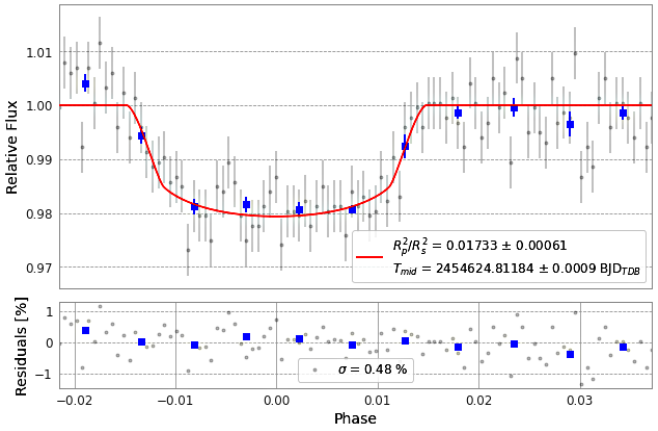

(f) 07 June 2008 (R)

Figure 5. XO-1b amateur contributed transit data and models: The red lines show the expected light variation based on the best fitting exotic model for each transit. The filters used are indicated by the text in brackets in the sub-figure captions: "B" is Johnson B, "R" is Johnson R, and "Clear" is no filter.

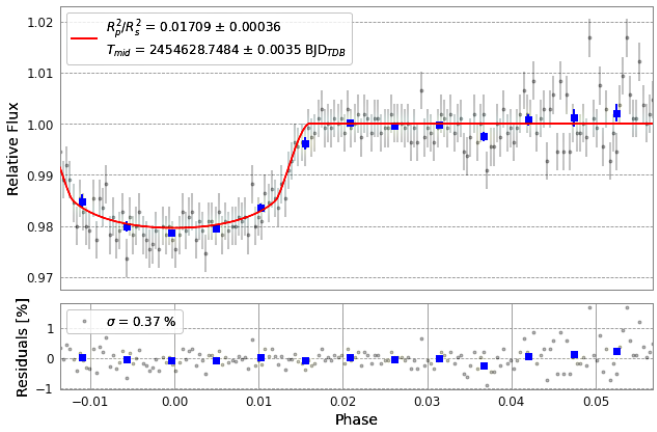

(g) 11 June 2008 (R)

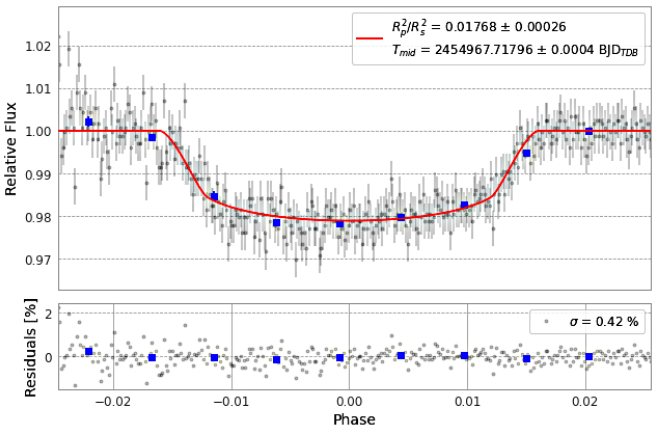

(j) 16 May 2009 (R)

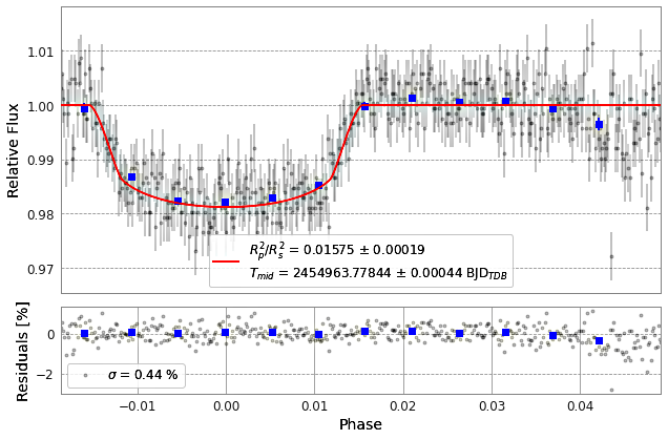

(h) 02 May 2009 (R)

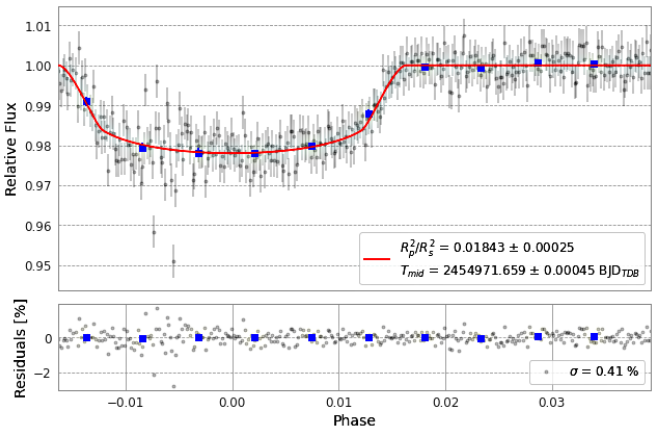

(k) 20 May 2009 (R)

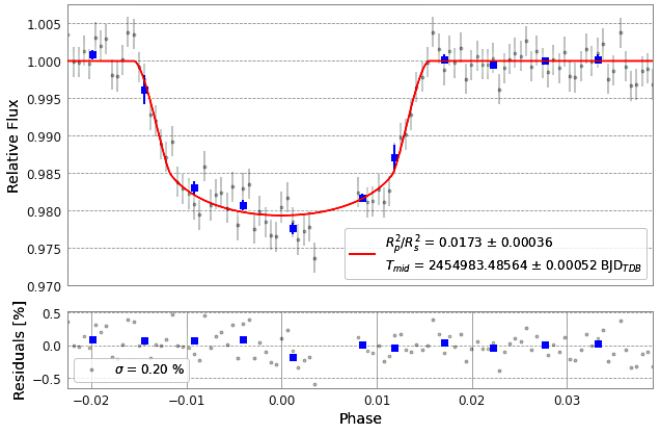

(i) 13 May 2009 (R)

Figure 5. XO-1b amateur contributed transit data and models, cont.

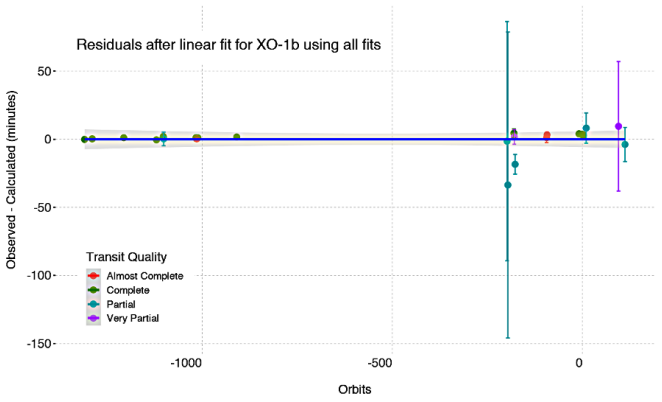

(a) All transits

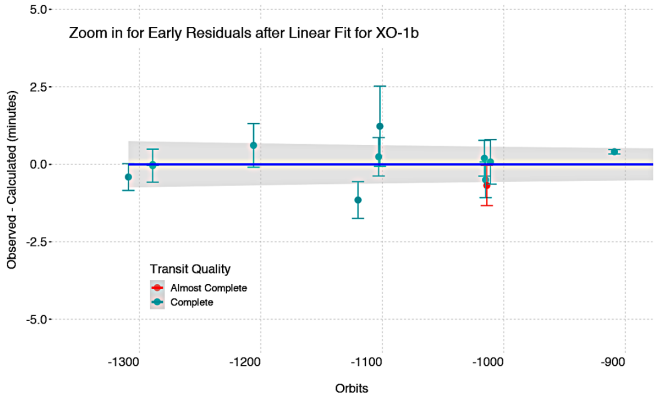

(c) Fits to early complete and near-complete transits

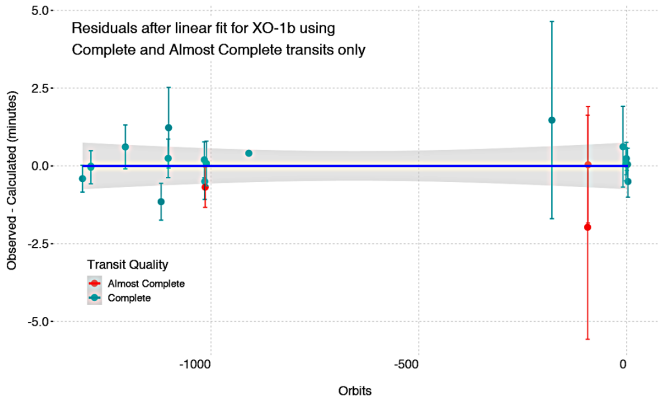

(b) Only complete and near-complete transits

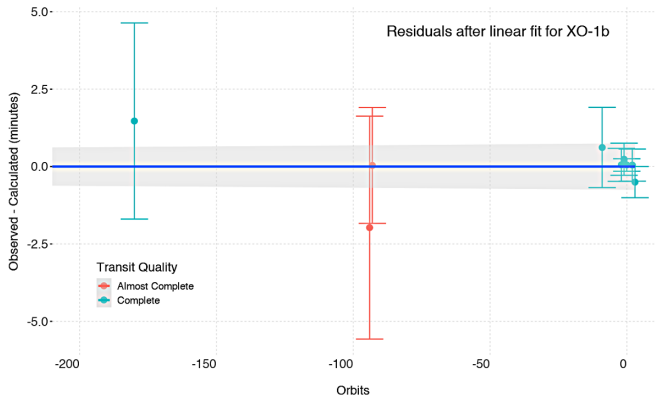

(d) Fits to late complete and near-complete transits

Figure 6. Regression fits to the mid-transit times. Sub-figure 6a shows the the residuals are a linear fit to the mid-transit timings. The grey shaded area plots the 3σ confidence range of a linear regression to these residuals. Sub-figure 6b is similar, but using only transits that were considered complete or nearly complete (see Table 1). Sub-figures 6c zooms into the early data in Sub-figure 6b, while 6d zooms into the more recent data.

radii are in good agreement with the literature. We applied Bayesian Optimization together with a simple transit model in order to estimate the orbital inclination, limb darkening, and radii. However, the implementation was too simple for a planet of the relative size XO-1b has to its host star, leading to recommendations on how to improve the modeling for further work.

A possible extension for projects similar to the current one could be to investigate combining observations from several transits together. EXOTIC outputs processed photometry, allowing users of this tool to explore this idea. Data would be phased by the orbital period (such as derived from a regression analysis as in this paper). The combined "transit" could then be analysed to see if the parameter estimates are better defined than in the analyses of the individual transits. This would need to include careful examination of the transit data to see if there were any additional variations in the data, such as might be caused by "star spots," and keeping to the same band passes across the data set.

This project is part of a wider effort, initially involving final year undergraduate (Honors) students in statistics at the National University of Singapore since 2012. Students found the exoplanet and variable star projects to be interesting and challenging, giving them the opportunity to develop an understanding of the scientific method, scientific programming skills (such as R, PYTHON, JULIA, AND FORTRAN), and documentation skills (including scientific publishing and LaTeX). The program was extended to a community college in the US, with similarly favorable results (see, e.g., Parker *et al.* 2021). Banks *et al.* (2020, and references therein) discussed the overall project and its benefits, which hopefully include increasing student interest in astronomy and science in general. They encouraged possible extension to high school students, leading to this particular project as a test case. We believe it confirms that such efforts are worthwhile, both at high school and undergraduate levels—which is supported by the success of other programs reported in this journal such as Stanford Online High School led by Kalée Tock (see, e.g., Bansal *et al.* 2022), the RR Lyrae star clusters project (see, e.g., Soper *et al.*, 2022) led by Dr. M. Fitzgerald (Edith Cowan University, Australia), and papers such as Kim and Percy (2022). There are sufficient astronomical databases and imagery available (or partnerships with active amateur astronomers could lead to interesting photometry or radial velocity based analysis projects), together with easy-to-run analysis tools such as EXOTIC, to create interesting and "bite sized" projects for such students. The workload of a project is an important consideration given that high school students must balance the research project with their high school studies, sporting activities, and college applications. Based on our experience, we strongly recommend projects such as the current

one as both interesting for the students, regardless of whether they advance to tertiary study in astronomy, and good for the future support of astronomy.

4. Acknowledgements

This publication makes use of the EXOTIC data reduction package from Exoplanet Watch (also known as Exowatch), a citizen science project managed by NASA's Jet Propulsion Laboratory (JPL) on behalf of NASA's Universe of Learning and which is supported by NASA under award number NNX16AC65A to the Space Telescope Science Institute. We thank the Harvard-Smithsonian Center for Astrophysics for the MicroObservatory (MObs) data kindly made available by Frank Sienkiewicz for this project. These data would be available on reasonable request to him. MObs data for individual transits can also be requested from the Exoplanet Watch website (https://exoplanets.nasa.gov/exoplanet-watch/how-to-contribute/data-checkout/). This research has made use of the NASA Exoplanet Archive, which is operated by the California Institute of Technology, under contract with the National Aeronautics and Space Administration under the Exoplanet Exploration Program. We thank the University of Queensland for collaboration software. This paper includes data collected by the TESS mission and obtained from the MAST data archive at the Space Telescope Science Institute (STScI). STScI is operated by the Association of Universities for Research in Astronomy, Inc., under NASA contract NAS 5-26555. We are grateful to the amateur astronomers who kindly placed their transit observations into the NEA for public access. We thank the anonymous referee for their comments and guidance which improved the paper.

References

Akeson, R. L., *et al.* 2013, *Publ. Astron. Soc. Pacific.*, **125**, 989.
Banks, T., Rhodes, M. D., and Budding, E. 2020, *South. Stars*, **59**, 17.
Bansal, A., Hamrick, P., and Tock, K. 2022, *J. Amer. Assoc. Var. Star Obs.*, **50**, 34.
Bonomo, A. S., *et al.* 2017, *Astron. Astrophys.*, **602**, 107.
Burke, C. J., *et al.* 2010, *Astrophys. J.*, **719**, 1796.
Carpenter, B., *et al.* 2017, *J. Statistical Software*, **76**, 1.
Croll B., *et al.* 2007, *Astrophys. J.*, **658**, 1328.
Eastman, J., Gaudi, B. S., and Agol, E. 2013, *Publ. Astron. Soc. Pacific*, **125**, 83.
Holman, M. J., *et al.* 2006, *Astrophys. J.*, **652**, 1715.
Kim, J. V. E., and Percy, J. R. 2022, *J. Amer. Assoc. Var. Star Obs.*, **50**, 178.
Kokori, A., *et al.* 2022, *Astrophys. J., Suppl. Ser.*, **258**, 40.
Mandel, K., and Agol, E. 2002, *Astrophys. J., Lett.*, **580L**, 171.
McCullough, P. R., *et al.* 2006, *Astrophys. J.*, **648**, 1228.
Ng, S. Y., Jiadi, Z., Püsküllü, Ç, Banks, T., Budding, E., and Rhodes, M. D. 2021, *J. Astrophys. Astron.*, **42**, 110.
North, A., and Banks, T. 2022, *J. Amer. Assoc. Var. Star Obs.*, **50**, 184.
Parker, R., Parker, L., Parker, H, Uddin, F., and Banks, T. 2021, *J. Amer. Assoc. Var. Star Obs.*, **49**, 178.
Patel, J. A., and Espinoza, N. 2022, *Astron. J.*, **163**, 228.
Ricker, G. R., *et al.* 2014, *Proc. SPIE*, **9143**, 914320 (DOI: 10.1117/12.2063489).
Sadler, P. M., *et al.* 2001, *J. Sci. Education Technol.*, **10**, 39 (DOI: 10.1023/A:1016668526933).
Soper, C., Tenenbaum, C., Lounsbery, A., Rheiner, J., and Klassen, D. 2022, *J. Amer. Assoc. Var. Star Obs.*, **50**, 28.
Southworth, J., 2010, *Mon. Not. Roy. Astron. Soc.*, **408**, 1689.
Stan Development Team. 2022, RStan: the R interface to Stan (http://mc-stan.org).
Stassun, K. G., Collins, K. A., and Gaudi, B. S. 2017, *Astron. J.*, **153**, 136.
Torres, G., Winn, J. N., and Holman, M. J. 2008, *Astophys. J.*, **677**, 1324.
Wilson, D. M., *et al.* 2006, *Publ. Astron. Soc. Pacific*, **118**, 1245.
Zellem, R. T., *et al.* 2020, *Publ. Astron. Soc. Pacific*, **132**, 054401 (DOI: 10.1088/1538-3873/ab7ee7).